Research Article | Vol. 32, No. 7 / 25 Mar 2024 / Optics Express 12783
Optics EXPRESS

Transient pump-probe analysis of pump-induced lensing in laser amplifiers

HUAIFENG XIAO,* XUNUO JIANG, AND MICHAEL J. DAMZEN

Photonics, The Blackett Laboratory, Dept of Physics, Imperial College London, Prince Consort Road, London SW7 2AZ, UK
huaifeng.xiao20@imperial.ac.uk

Abstract: Understanding of pump-induced lensing in laser amplifiers is essential for the optimized design of high-power lasers with high spatial quality, but there is usually incomplete knowledge of the interplay between thermal and population induced lensing mechanisms, lensing under lasing and non-lasing conditions, and transient lensing effects under pulsed operation. This paper provides quantitative insight of pump-induced lensing effects by using experimental transient pump-probe measurements in an alexandrite laser amplifier end-pumped by a short pulse pump beam with Gaussian spatial intensity distribution. Lensing results are presented showing a large difference in lensing under both non-lasing and lasing conditions and distinction of the population lens and thermal lens contributions from their different response time. Different pump beam sizes are used to show the variation of the relative strength of the lensing mechanisms. Comparison of experimental results with the analytical transient theory developed in this paper for the Gaussian pump beam gives excellent agreement and quantitative information on the thermal and population contributions to the amplifier lens. This paper provides a methodology for quantitative investigation of pump-induced lensing in general laser amplifier systems, and potentially other classes of optical materials with residual optical absorption.

Published by Optica Publishing Group under the terms of the Creative Commons Attribution 4.0 License. Further distribution of this work must maintain attribution to the author(s) and the published article's title, journal citation, and DOI.

1. Introduction

Pump-induced lensing in a laser gain medium is one of the main limits to power scaling of laser systems. As pump power is increased, the increasing lensing strength in the gain medium can negatively impact the cavity design, dynamically changing its stability range, and altering the fundamental mode size which, together with lensing aberrations, leads to degradation in laser beam quality. The primary physical mechanism usually considered is thermally-induced lensing due to heat deposited in the gain medium by the pump excitation [1]. This thermal lens results from the temperature-dependence of the medium refractive index (dn/dT) and in a solid-state medium can have further contributions from the surface bulging and photo-elastic effect due to differential expansion and strain [2]. Many solid-state gain media have also been found to display an inversion-dependent refractive index change caused by the difference in the polarizability of excited and ground state ions leading to what is often referred to as a population lens [3]. The population component of the pump-induced lens has been relatively neglected in consideration of amplifier lensing in the literature and is almost unmentioned in laser textbooks. This is even though the population mechanism has been shown to occur in many classes of solid-state gain media including the important classes of Nd-doped crystals [3–6], Cr-doped crystals [7–11], and Yb-doped crystals [12–14], and the population-induced refractive index change Δn_p can even dominate over the thermally-induced refractive index change Δn_T in some gain media [6]. This means that induced lensing based solely on thermal mechanisms can lead to imprecise calculated lensing or lensing measurements can infer wrong thermal properties. In pulsed laser systems, this incomplete consideration of pump-induced mechanisms can be much worse as the

#519582 https://doi.org/10.1364/OE.519582
Journal © 2024 Received 23 Jan 2024; revised 8 Mar 2024; accepted 12 Mar 2024; published 21 Mar 2024

Optics EXPRESS

population lens mechanism based in inversion will usually operate on a much faster timescale than the slower thermal diffusion lensing process. Self-Q-switching has been observed in some lasers [15–16] for which the only plausible explanation is hypothesized to be caused by the fast modulation of the population lens. Hence, it is important for optimize and control of this pulsing (or to avoid it) to have rigorous information and be able to make distinction between different lensing mechanisms and their relative impact.

Many experimental methods have been employed for determining pump-induced lensing in laser amplifiers [17]. One common but indirect technique is to measure mode size from the output of a laser cavity and together with an ABCD cavity analysis to infer the lensing power of the gain medium [18]. However, this technique (like many others) is a steady-state method and does not discrimination between different lensing mechanisms. This method also cannot provide lensing information on the non-lasing amplifier case, that might be required if gain medium is used as a power amplifier. Alternatively, time-resolved measurements do provide a potential means to discriminate between different lensing mechanisms by their different response times, usually characterized by a relatively fast inversion population dynamics $N(t)$ and slower thermal diffusion timescales governed by the heat-diffusion equation for the spatio-temporal variation of the medium temperature distribution $T(\underline{r}, t)$. Time-resolved studies have been performed on pump-induced refractive index changes $\Delta n(t)$ in laser amplifier media using interferometry and Z-scan methods [3,12]. These methods can quantify the polarizability difference between the excited and ground state electronic population if the inversion population can be calculated but they do not directly provide lensing data that are needed for laser cavity design and understanding of laser performance. Direct pump-induced lensing measurement can be made by wavefront sensing using a probe beam and lateral shearing interferometry [19] or a Shack-Hartmann wavefront sensor [2,10]. Shack-Hartmann wavefront sensors (SH-WFS) are particularly good due to their accurate determination of wavefront curvature but the time response to compute the wavefront is too slow to directly supply fast transient information on the sub-millisecond timescale.

In this work, we perform experimental time-resolved pump-probe measurement of the transient growth and decay of the pump-induced lens in a laser amplifier combined with some new analytical theory of the temporal dynamics of the thermal and population lens mechanisms. Our experimental method uses a repetitively pulsed pump beam (pump duration, t_p) with Gaussian spatial intensity distribution $I_p(\underline{r})$ to end-pump a gain medium (alexandrite crystal) and a time-delayed short (nanosecond) probe pulse with a time-gated Shack-Hartmann wavefront sensor (SH-WFS) to directly monitor the transient variation of the dioptric power of the pump-induced lens $D(t) = 1/f(t)$ with high temporal resolution. The analytical theory of this paper is developed for the transient thermal $D_T(t)$ and population $D_P(t)$ lens components for the Gaussian end-pumping case for both growth and decay of the lensing under short-pumping pulse conditions. The development of these analytical solutions is shown in this paper to support quantitative interpretation of the experimental measurements.

2. Theoretical analysis of transient pump-induced lensing

For the theoretical analysis, we consider an "ideal" four-level gain medium system, as shown in Fig. 1, with upper laser level population distribution $N(r, z, t)$ and in which the lower laser level population remains zero due to a fast relaxation to the ground state. The gain medium is considered as a cylindrical rod with end pumping centred at radial coordinate ($r = 0$) and incident at its end face ($z = 0$) by a pump beam with Gaussian spatial intensity profile:

$$I_p(r, z, t) = \frac{2P(t)}{\pi w_p^2} e^{-2(r^2/w_p^2)} e^{-\alpha_p z} \tag{1}$$

Optics EXPRESS

with waist size w_p, pump absorption coefficient α_p, and pump power $P(t)$ taken as a square pulse with constant power P and duration t_p. We develop an analytical theory of the transient pump-induced lens formed in the gain medium with dioptric power $D(t) = 1/f(t) = D_T(t) + D_P(t)$ modelled as a combined thermally-induced lens $D_T(t)$ and an inversion-induced (population) lens $D_P(t)$. The thermal lens is formed by some fraction η_H of the absorbed pump power being converted to heat producing a temperature distribution $T(r, z, t)$ and related thermal refractive index change $\Delta n_T(r, z, t)$. In the thermal analysis we account for heat input coming in two steps after a pump photon is absorbed (see Fig. 1): an immediate upper-level heating factor $\eta_{H1} = \beta\eta_H$ (with partial fraction β of the quantum defect) due to fast non-radiative relaxation from the pump level to the upper laser level, followed by a delayed lower-level heating factor $\eta_{H2} = (1 - \beta)\eta_H$ by non-radiative decay of the lower laser level to the ground-state after spontaneous emission. The population lens is formed by the polarizability of excited state ions (α_e) and ground state ions (α_g) being different ($\Delta\alpha_p = \alpha_e - \alpha_g$) and the population distribution $N(r, z, t)$ resulting in a population refractive index change $\Delta n_P(r, z, t)$.

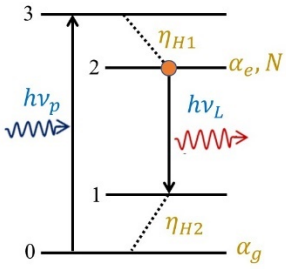


Fig. 1. Four-level laser amplifier system with combined thermally-induced lensing and population lensing.

2.1. Thermally-induced lens, $D_T(t)$

Heat deposition in the gain medium by the absorption of the pump beam results in a spatio-temporal evolution of the temperature governed by the transient heat diffusion equation: $\frac{\rho C_p}{\kappa}\frac{\partial T}{\partial t} = \nabla^2 \mathrm{T} + \frac{Q}{\kappa}$ where $T(\underline{r})$ is temperature, $Q(\underline{r})$ is heating power per unit volume, and κ, ρ, C_p are the medium thermal conductivity, density, and specific heat capacity, respectively. In cylindrical coordinates with axially-symmetric heating $Q(r, z)$, where r and z are transverse radial and axial coordinates, respectively, the heat equation can be written as:

$$\frac{\partial T}{\partial t} = \frac{\alpha}{r}\left[\frac{\partial}{\partial r}\left(r\frac{\partial T}{\partial r}\right)\right] + \alpha\frac{Q}{\kappa} \tag{2}$$

where $\alpha = \kappa/\rho C_p$ is thermal diffusivity, and we have neglected axial (z) second derivative assuming heat flow is predominantly in transverse radial direction. This is a realistic approximation for an end-pumped case with pump waist size small compared to absorption depth in the amplifier ($w_p \ll 1/\alpha_p$) which is commonly valid, as is the experimental case of this work ($w_p \approx 0.2$ mm; $1/\alpha_p \approx 2$ mm). A Gaussian optical pump beam (Eq. (1)) produces a Gaussian heating distribution $Q(r, z, t) = \eta_H\alpha_p(2P(t)/\pi w_p^2)e^{-2(r^2/w_p^2)}e^{-\alpha_p z}$ where heat factor η_H is fraction of absorbed pump power converted to heat power.

In most theory of pump-induced lensing, the heat factor η_H is taken as the quantum defect, $\eta_D = 1 - \lambda_p/\lambda_L$, the fractional difference between the absorbed pump photon energy at wavelength λ_p and the emitted spontaneous (or stimulated) emission photon energy at wavelength λ_L. However, this commonly used assumption is not strictly true at short timescales as the heat

Optics EXPRESS

comes in two steps, and we use this two-step approach in this analysis. After absorption of a pump photon, there is an instantaneous upper-level heating factor $\eta_{H1} = \beta\eta_H$, followed by a delayed lower-level heating factor after spontaneous emission $\eta_{H2} = (1-\beta)\eta_H$, as indicated in Fig. 1. This produces a time-dependent heating rate $Q(t)$ which is the sum of the rates of pumping and spontaneous emission weighted by their respective partial heating factors: $Q(t) = \eta_H[\beta\alpha_p I_p + (1-\beta)h\nu_p N(t)/\tau]$ where τ is upper-state lifetime and $h\nu_p$ is pump photon energy. Using the solution of rate equation for upper-state population $N(t) = \alpha_p I_p \tau/h\nu_p(1-e^{-t/\tau})$ during pumping pulse, we obtain $Q(t) = \alpha_p I_p \eta_H[\beta + (1-\beta)(1-e^{-t/\tau})]$ from which we can identify a time-dependent heating factor:

$$\eta_H(t) = \eta_H\left[\beta + (1-\beta)\left(1-e^{-\frac{t}{\tau}}\right)\right]. \tag{3}$$

For short times ($t \ll \tau$), only the upper-heating factor is important $\eta_H(t) = \beta\eta_H$ but heating factor increase with time and at long times ($t \gg \tau$) reaches its quantum defect value $\eta_H(t) = \eta_H$ when in steady-state the rates of pump-inversion and spontaneous emission are equal.

For pumping on short timescales when thermal diffusion can be neglected, the medium temperature given by Eq. (2) increases due to the integrated heat input $T(r,z,t) = \frac{\alpha}{\kappa}\int_0^t Q(r,z,t')dt' = \frac{\alpha}{\kappa}\alpha_p I_p \eta_H\{\beta t + (1-\beta)[t-\tau(1-e^{-t/\tau})]\}$ and has the same Gaussian spatial distribution as the pump beam $I_p(r,z) = \frac{2P}{\pi w_p^2}e^{-2(r^2/w_p^2)}e^{-\alpha_p z}$. The pump-induced change in optical path length $W(r,t)$ is found by integrating over the amplifier length (l) and given by:

$$W(r,t) = \left(\frac{dn}{dT}\right)\frac{2\eta_H \alpha P_a}{\kappa\pi w_p^2}[t-(1-\beta)\tau(1-e^{-t/\tau})]e^{-2(r^2/w_p^2)} \tag{4}$$

where (dn/dT) is the thermo-optic coefficient that relates temperature to refractive index change, and $P_a = P(1-e^{-\alpha_p l})$ is the absorbed pump power. The thermo-optic coefficient is the major heat-induced lensing effect but can be modified $(dn/dT)_{eff}$ to include lensing contributions due to end-face bulging and strain-induced photoelastic effect, but these together add usually small relative contribution (~10-20%) [10]. The axial dioptric strength of thermally-induced lens is given by $D_T(t) = \frac{1}{f_T(t)} = -\frac{1}{r}\left.\frac{dW(r,t)}{dr}\right|_{r=0}$, leading to transient dioptric thermal lens:

$$D_T(t) = \left(\frac{dn}{dT}\right)\frac{8\eta_H \alpha P_a}{\kappa\pi w_p^4}[t-(1-\beta)\tau(1-e^{-t/\tau})] \tag{5a}$$

Using the steady-state axial thermally-induced lensing solution for a Gaussian pump beam $D_{T,SS} = \left(\frac{dn}{dT}\right)\frac{\eta_H P_a}{\kappa\pi w_p^2}$ [10], the transient thermal lensing formula, we can also be written in a more convenient form:

$$D_T(t) = D_{T,SS}\frac{[t-(1-\beta)\tau(1-e^{-t/\tau})]}{t_0} \tag{5b}$$

where the quantity $t_0 = w_p^2/8\alpha$ is a characteristic thermal diffusion response time for a Gaussian pump size w_p. Equation (5b) provides the thermal lensing during the pumping and valid with neglect of transverse heat diffusion for short pumping time $t \ll t_0$.

After the end of the pump pulse at time $t = t_p$ there is still a fraction of heat stored in the upper-state population $N(t_p) = \alpha_p I_p \tau/h\nu_p(1-e^{-t_p/\tau})$ that is release by spontaneous emission at a rate $Q(t) = \eta_H(1-\beta)(h\nu_p/\tau)N(t_p)e^{-t/\tau}$, where time t is with respect to end of pump pulse. Inclusion of this heating, again with neglect of thermal diffusion, leads to decay of thermal lens

Optics EXPRESS

$D_T(t)$ at time t after pump pulse:

$$D_T(t) = D_{T,SS}\frac{[t_p - (1-\beta)\tau(1-e^{-t_p/\tau})e^{-t/\tau}]}{t_0}. \tag{5c}$$

The quantity $(1-\beta)\tau(1-e^{-t_p/\tau})$ in Eq. (5c) is proportional to the stored heat in the medium which is released at an exponential (spontaneous) decay rate after end of pump pulse.

We now consider the case after the pump is switched off (and any residual heat release) and $Q = 0$ in the transient heat diffusion equation. The general solution of the heat diffusion in this case is given by [20]:

$$T(\underline{r}, t) = \frac{1}{8(\pi\alpha t)^{3/2}}\int T_0(\underline{r}')\exp -\left[\frac{(\underline{r}-\underline{r}')^2}{4\alpha t}\right]d^3x' \tag{6}$$

where $T_0(\underline{r}')$ is the initial temperature profile at $t = 0$, and there is a triple integral over a general 3-D coordinate system. The integral has no general solution, but a special case solution can be found when the initial temperature profile is a point source (mathematically, the Dirac delta function, $\delta(\underline{r})$). For radial heat diffusion into a 2-D cylindrical coordinate system with initial temperature profile $T_0(r, z) = T_0(z)\delta(r)$, which can be considered a line of point sources along the z-axis, the form of the transient solution is [20]:

$$T(r, z, t) = \frac{A_0(z)}{t}\exp -\left(\frac{r^2}{4\alpha t}\right). \tag{7}$$

The temperature at any z-coordinate evolves in time as a Gaussian distribution $T(r, t) = A(t)\exp -(r^2/w(t)^2)$ with an expanding width $w(t) = \sqrt{4\alpha t}$, and decaying amplitude $A(t) = A_0/t$, but with overall conservation of energy of the total medium heat stored in the distribution. This solution is helpful to understand the mathematical form of the transient temperature evolution, but a point source is not a realistic initial temperature distribution at time $t = 0$ for the finite pump beam size used in the medium. However, we can perform a mathematical "trick" by knowing the initial temperature distribution $T_0(r, z)$ has a Gaussian transverse form (or could be approximated to one) at $t = 0$. We find an offset time t_0 when the delta function solution (Eq. (7)) produces a Gaussian distribution with transverse size matching the known initial Gaussian temperature distribution produced by the short pump pulse with Gaussian pump size w_p:

$$T_0(r, z) = T_0\exp -2\left(\frac{r^2}{w_p^2}\right)e^{-\alpha_p z}. \tag{8}$$

Matching Gaussian exponents in Eqs. (7) and (8), $4\alpha t_0 = w_p^2/2$ provides an offset time given by

$$t_0 = \frac{w_p^2}{8\alpha}. \tag{9}$$

This is the same characteristic thermal response time we found previously for neglect of transverse diffusion in the transient solution of Eq. (5(b)). Knowing the initial Gaussian temperature distribution is the same as would have been produced by a delta-function heat impulse after a time $t = t_0$, we also know this Gaussian distribution will evolve as an expanding Gaussian at later times by using Eq. (7) with a shifted time coordinate $t' = t + t_0$, where time t is relative to end of pump pulse, with solution given by

$$T(r, t' = t + t_0) = \frac{A_0}{t'}\exp -\left(\frac{r^2}{4\alpha t'}\right) t \geq 0. \tag{10}$$

Following same procedure in Eqs. (4) and (5), we can use the expanding temperature profile to obtain the evolving optical path length $W(r, t)$ and derive a transient dioptric power of decaying

Optics EXPRESS

thermal lens $D_T(t)$ after the end of the pulsed pump. It is given by,

$$D_T(t) = D_T(0)\frac{t_0^2}{t'^2} = \frac{D_T(0)}{[1 + (t/t_0)^2]};\ t \geq 0 \tag{11}$$

where $D_T(0)$ is the initial dioptric thermal lens power at end of pump pulse.

2.2. Population lens, $D_P(t)$

The rate equation for the upper-laser population $N(r, z, t)$ of an ideal four-level laser transition is given by:

$$\frac{dN(r,z,t)}{dt} = \frac{\alpha_p I_p(r,z)}{h\nu_p} - \frac{N(r,z,t)}{\tau} \tag{12}$$

where $h\nu_p$ is pump photon energy, h is Planck's constant, ν_p is pump frequency, and τ is upper-state lifetime. It has solution during a pumping pulse with constant power:

$$N(r,z,t) = \frac{\alpha_p I(r,z)\tau}{h\nu_p}[1 - e^{-t/\tau}] \tag{13}$$

The relationship between upper-state population N and refractive index change Δn_p is given by [10,13]

$$\Delta n_p(r,z) = C.\frac{N(r,z)}{N_T} \tag{14}$$

where $C = 2\pi f_L^2 N_T \Delta\alpha_p/n_0$, $\Delta\alpha_p = \alpha_e - \alpha_g$ is the polarizability difference of the excited and ground state ions, n_0 is the unperturbed refractive index, $f_L = (n_0^2 + 2)/3$ is the Lorentz factor, and N_T is the total laser active population density. Following a similar analysis as used for the thermally-induced lens for the change in optical path length $W(r, t)$, we can derive from Eqs. (13) and (14) the transient dioptric population lens formed by a Gaussian pump beam:

$$D_P(t) = \frac{1}{f_P} = \frac{8CP_a}{\alpha_p \pi w_p^4 I_S}[1 - e^{-t/\tau}] = D_{P,SS}\,[1 - e^{-t/\tau}] \tag{15a}$$

where $P_a = P(1 - e^{-\alpha_p l})$ is the absorbed pump power, $I_S = h\nu_p/\sigma_p\tau$ is the saturation intensity for absorption, σ_p is the absorption cross-section, and $D_{P,SS}$ is the steady-state population lens as $t \to \infty$.

After pumping pulse duration t_p, the population lens decays exponentially according to

$$D_P(t) = D_{P,SS}[1 - e^{-t_p/\tau}]e^{-t/\tau} \tag{15b}$$

where time coordinate t in Eq. (15b) is redefined as relative to end of pump pulse.

2.3. Combined thermal and population lens

During pump pulse for short time $t \ll t_0$, when thermal diffusion can be neglected and with time t relative to start of pumping, the combined thermal lens power (Eq. (5b)) and population lens power (Eq. (15a)) is given by:

$$D(t) = D_T(t) + D_P(t) = D_{T,SS}\frac{[t - (1-\beta)\tau(1 - e^{-t/\tau})]}{t_0} + D_{P,SS}\,[1 - e^{-t/\tau}] \tag{16}$$

where $D_{T,SS} = \left(\frac{dn}{dT}\right)\frac{\eta_H P_a}{\kappa\pi w_p^2}$, $D_{P,SS} = \frac{8CP_a}{\alpha_p\pi w_p^4 I_S}$, and $t_0 = w_p^2/8\alpha$.

Optics EXPRESS

For very short times $t \ll t_0, \tau$, the initial combined dioptric lens grows linearly in time:

$$D(t) = \left(\frac{D_{T,SS}.\beta}{t_0} + \frac{D_{P,SS}}{\tau}\right) t \tag{17}$$

The decay of dioptric power of combined thermal and population lens when pumping is ended is given by Eqs. (5c) and (15b)

$$D(t) = \frac{D_T(0)}{[1 + (t/t_0)^2]} + D_P(0)e^{-t/\tau} \tag{18}$$

where $D_T(0) = D_T(t_p)$ from Eq. (5b) and $D_P(0) = D_{P,SS}[1 - e^{-t_p/\tau}]$ from Eq. (15).

3. Experimental setup

Figure 2 shows the experiment setup used for the transient pump-probe measurements of an end-pumped gain medium. The gain medium in this study was alexandrite end-pumped by a pulsed diode laser and using a short pulse probe beam to directly monitor the time-evolution of the pump-induced lens with a Shack-Hartmann wavefront sensor (SH-WFS).

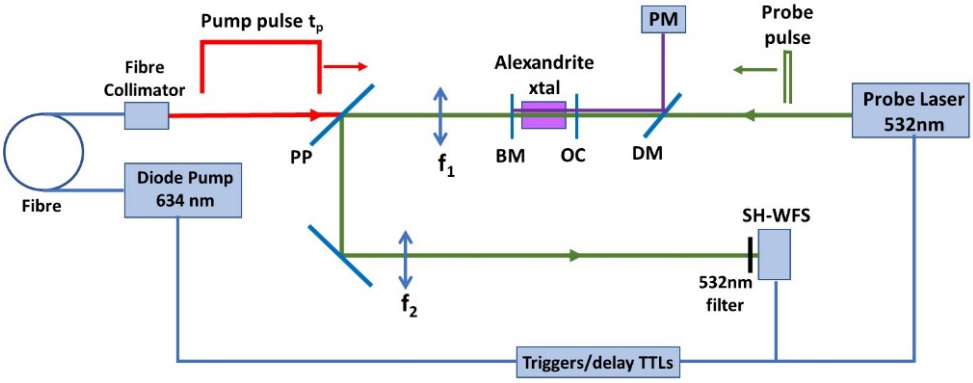


Fig. 2. Schematic of the experimental system for transient pump-probe measurement of pump-induced lensing in laser gain medium (alexandrite) under non-lasing and lasing conditions

The fibre-delivered laser diode pump module with wavelength 634 nm was operated by a pulsed diode driver to produce a square pump pulse with controllable duration t_p at a pulse repetition frequency of 50 Hz. Its output was transmitted through a plate polarizer (PP) to give linear polarization that was matched to the high absorbing b-axis of alexandrite. The pump beam was focused onto the alexandrite crystal end face with pump lens f_1. The spatial beam quality of the pump was measured as $M^2 = 70$ and its spatial form had near Gaussian intensity profile. Its beam size w_p at the crystal was measured for each pump lens used. From crystal transmission measurements, the pump absorption coefficient $\alpha_p = 560\ m^{-1}$ was deduced.

The alexandrite laser crystal was a plane-plane rod with 4 mm diameter, 8 mm length, and 0.22 at.% Cr doping and mounted in a temperature-controlled copper holder. To investigate pump-induced lensing under lasing conditions, the alexandrite crystal was placed in a laser cavity consisting of a back mirror BM (high reflectivity at laser wavelength $\lambda_L = 760$nm and high transmission at pump wavelength $\lambda_p = 634$nm) and an output coupler OC (reflectivity $R_{OC} = 99\%$ at laser wavelength $\lambda_l = 760nm$). The length of the laser cavity was $L_C = 18$mm. The alexandrite laser output was taken to a power meter (PM) via reflection from a dichroic mirror (DM) which transmitted the probe beam and isolated the probe laser from the alexandrite

Optics EXPRESS

laser system. Pump-induced lensing under non-lasing conditions was measured by misaligning the output coupler (OC) to suppress lasing.

The short pulse probe beam (λ_{pr} = 532nm) was generated by an in-house built Q-switched Nd:YVO_4 laser which was frequency-doubled by an LBO crystal. It had 11 ns pulse duration. A pair of lenses was used to provide a near to plane probe wavefront at the laser crystal and adjust its size ($2w_{pr} = 1.3mm$) to overfill the pump region in the crystal. The probe beam wavefront after passing through the laser crystal is reshaped by the pump-induced lensing and was then relay imaged by pump lens f_1 and a second lens f_2 = 300mm onto a Shack-Hartmann wavefront sensor, SH-WFS (Thorlabs, WFS20-7AR/M). The imaging magnification was $m = -f_2/f_1$ and the lens combination was chosen to match the pump region size to the chosen sensor pupil size for good measurement accuracy by covering sufficient micro-lenslet elements (with separation 150 µm) and range of wavefront curvatures to be measured. A green 532 nm bandpass filter was used to reject any residual pump wavelength or alexandrite lasing or spontaneous emission. The SH-WFS was operated in a time-gated mode with trigger timed to measure the radius of curvature (RoC) at the sensor for each individual probe pulse. The probe laser was operated at same pulse rate as the pump laser (50 Hz) and with controlled timing delay of the probe pulse relative to the start of the pump pulse. This made it possible to map the time evolution of the transient pump-induced lensing $f(t)$ in the laser crystal with repetitive pumping. The induced transient lens in the laser crystal was calculated from the formula $f(t) = (RoC(t))/m^2$ from the $RoC(t)$ SH-WFS measurements, which were averaged over 100 pulses for each time delay.

4. Experimental results

4.1. Steady-state pump-induced lensing measurements

As an initial study, the dioptric lensing in alexandrite gain medium was measured under steady-state pumping conditions using a continuous-wave pump beam (λ_p = 636 nm) with Gaussian spatial distribution and a continuous wave probe at wavelength 532 nm onto the Shack-Hartmann wavefront sensor (SH-WFS). The pump was supplied by the fibre-coupled red-diode laser module (operating in continuous-wave mode) described in Section 3 with a focusing lens f_1 = 50 mm, producing a minimum waist size w_p = 0.14 mm. Due to finite pump divergence over the laser crystal, an effective beam size $w_{p,e}$ is defined using the mean squared beam size w_p^2 weighted by the exponentially-absorbed pump intensity, $w_{p,e}^2 = \int_0^l e^{-\alpha_p z} w_p^2(z) dz / \int_0^l e^{-\alpha_p z} dz$ [21], giving $w_{p,e}$ = 0.167 mm.

Figure 3 shows the measured dioptric lensing power $D(m^{-1})$ as a function of absorbed pump power under both non-lasing conditions (black data) and lasing conditions (red data) as well as the lasing output power (green data). The non-lasing lensing has a near-linear dependence with absorbed pump power. Under lasing conditions, the lensing strongly diverges from the non-lasing case with much lower lensing strength after the onset of lasing. This strong difference between lasing and non-lasing pump-induced lensing was seen in a previous investigation of diode-pumped alexandrite by our group [10] and explained by hypothesizing that the lensing is a combination of a thermal lens and population lens components that is clamped under lasing conditions.

4.2. Transient pump-probe pump-induced lensing results

One aim of using pulsed pump and probe lensing measurements is to confirm the presence of the population lens by its different temporal signature to the thermal lens. This section presents some key results of this investigation of the transient lensing together with analysis and modelling based on the theory of Section 2 of this paper.

Optics EXPRESS

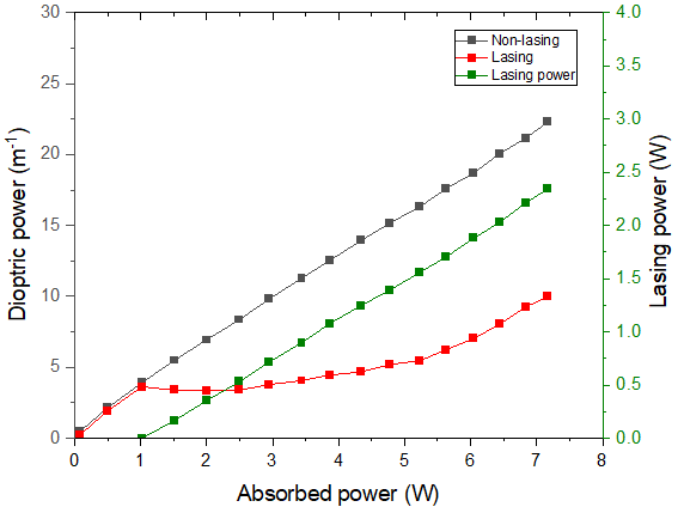


Fig. 3. Measured steady-state lensing dioptric power under non-lasing (red) and lasing (green) conditions, and lasing power (black) as function of the absorbed pump power.

Figure 4 shows the results of the measured temporal evolution of pump-induced lens for a relatively long pump pulse with pump duration t_p = 4 ms, operating at 50 Hz pulse rate (20 ms between pump pulses). The same red diode-pump was used as in the steady-state case with absorbed pump power 7.47 W (during the pulse on-time) and focusing lens f_1 = 50 mm, producing minimum waist size w_p = 0.14 mm, and effective beam size $w_{p,e}$ = 0.167 mm.

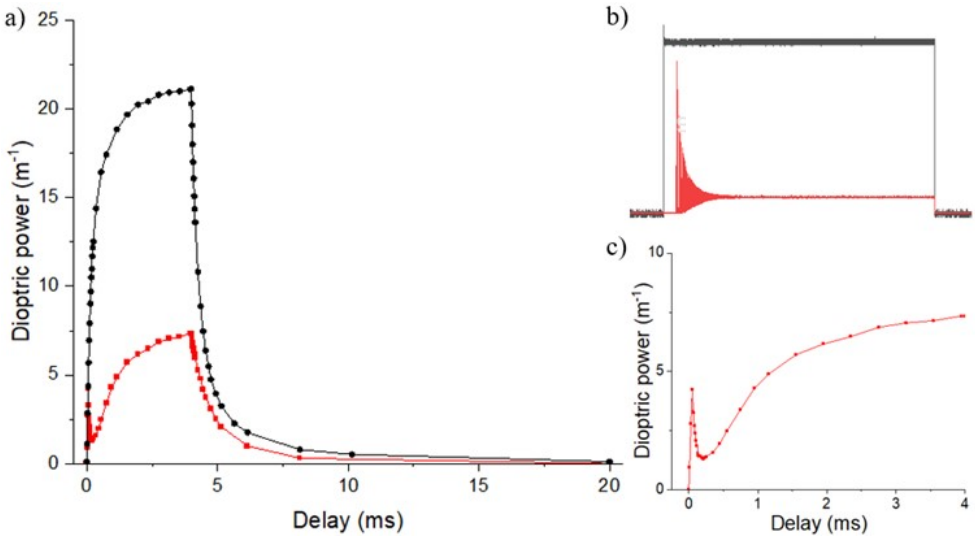


Fig. 4. a) Transient pump-induced lensing and its decay for a 4 ms pump pulse, under non-lasing conditions (black data) and lasing conditions (red data), b) shows example of a transient lasing pulse with relaxation oscillation (red trace), and c) is an enlargement of the early part of the lasing lens.

Figure 4(a) shows the time evolution of the dioptric lensing power $D(t)$ for both the non-lasing amplifier (with only spontaneous emission) and the lasing amplifier in an aligned lasing cavity

Optics EXPRESS

(with combined spontaneous and stimulated emission). With this "long" duration pump the pump-induced lens approaches quasi-steady-state at the end of the pump. For non-lasing the quasi-steady-state dioptric lensing power is ~ 21 m^{-1} in agreement with the steady-state lensing data for the CW pump in Fig. 3. The lensing decays to near zero (~0.1 m^{-1}) after 20 ms when the next pump pulse arrives, so each pump pulse can be considered independently. Under lasing conditions, the pump-induced lensing has a much lower quasi-steady-state value ~ 7 m^{-1}. Figure 4(b) shows the transient lasing output power has an initial period of relaxation oscillation evolving to a steady state. The dioptric powers under lasing and non-lasing cases follow the same initial increase up to ~ 4 m^{-1} until the first relaxation oscillation output occurs from the laser cavity (~ 60 µs after pumping starts) when the dioptric power drops to ~ 1.5 m^{-1} for the lasing case, as shown in the enlarged Fig. 4(c) for the non-lasing lensing.

The rapid drop in dioptric lens power cannot be explained by a slow thermal lensing mechanism but is fully consistent with the presence of an inversion-induced (population) lens. After the gain medium reaches threshold inversion for the laser cavity, there is a transient build-up of the intracavity flux during which time the inversion has grown above threshold value. The first relaxation oscillation depletes the inversion below threshold, and there follows further oscillation of laser output and inversion until steady-state is reached. The lensing follows a step-wise drop in the population component of the lens to its clamped population lens value at threshold inversion together with a slow transient growth of the thermal component of the lens. The transient pump-induced lens is therefore fully explained, at least in a qualitative sense, by this combined thermal and population lens model. The significant decrease in lensing under lasing seen in Fig. 4 with clamped population lens indicates that the majority contribution of the pump-induced lens under non-lasing conditions is the population lens in this case.

To investigate the impact of beam pump size, the transient pump-induced lensing was measured using three different pump lenses (f_1 = 50 mm, 60mm, and75mm) producing different effective pump sizes ($w_{p,e}$ = 0.167 mm, 0.182 mm, and 0.215 mm, respectively) all at the same 7.47W absorbed pump power and 4 ms pump duration. Figure 5 shows the results for these three cases. With increasing pump waist size, the quasi steady-state lensing strength reduces as expected due to decreased intensity and weaker curvature of the induced refractive distribution.

In these measurements, the pump duration t_p = 4 ms was longer than calculated time constant t_0 = 600 μs from Eq. (9). Large amount of diffusion will have occurred to increase the thermal extent to much larger than the input pump size and makes the time constant larger than t_0 for the subsequent lensing decay after pump is switched off. The experimental transient decay of the lens $D(t)$ after the pump pulse stops in the three cases of Fig. 5 was fitted with the function in Eq. (19) with a larger time constant t_T to extract information on the relative contribution of the thermal and population lens in these three cases:

$$D(t) = \frac{D_T(0)}{[1 + (t/t_T)^2]} + D_P(0)e^{-t/\tau} \tag{19}$$

where $D_T(0)$ and $D_P(0)$ are the initial thermal and population lens strengths in the fitting when the 4 ms pump pulse stops (taken as time $t = 0$), τ = 260 μs is the known upper-state lifetime for alexandrite at 25°C [22], and t_T is a time constant for the (slower) decay of the thermal component of the lens. The results of the fitting for the relative contributions of the thermal and population lens are summarized in Table 1. The value t_T ~ 1.5 ms was found in the fitting. For the smallest pump size (0.167 mm), the induced lens is dominated by the population lens which is 77% is the total lens. The relative contribution of the population lens decreases with larger pump size, with a value of 65% of the total lens for the largest pump size (0.215 mm). This relative decrease of the population lens is consistent in trend with the theoretical modelling since the steady-state thermal lens scales as $D_{T,SS} \propto 1/w_p^2$, whereas the steady-state population lens scales as $D_{P,SS} \propto 1/w_p^4$. This difference in scaling is due to the local nature of the population lens

Optics EXPRESS

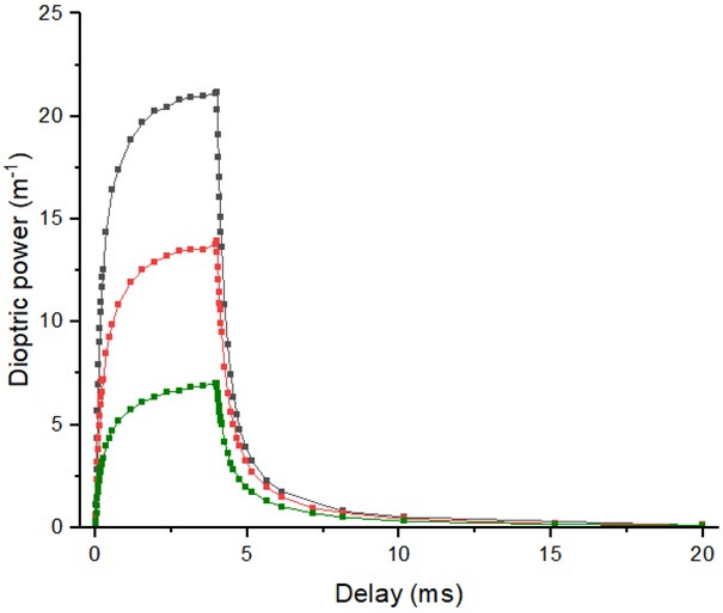


Fig. 5. Transient pump-induced lensing under non-lasing conditions for a 4 ms pump pulse with different effective pump waist sizes $w_{p,e}$: 0.167 mm (black data); 0.182 mm (red data); 0.215 mm (green data).

formed directly from the Gaussian population distribution, whereas the thermal lens is formed by a larger non-local steady-state radial temperature distribution following thermal diffusion.

Table 1. Fitted data for relative contribution of thermal and population lens component to pump-induced lens

Effective pump waist size ($w_{p,e}$)	Total Lens D (m^{-1})	Thermal Lens D_T (m^{-1})	Population Lens D_P (m^{-1})
0.167 mm	20.8	4.7	16.1
0.182 mm	13.7	4.2	9.5
0.215 mm	6.9	2.4	4.5

Figure 6 shows transient modelling of build-up and decay of the thermal lens (blue), population lens (green) and combined theoretical lens (black) for a long (4 ms) pump pulse and comparison to the experimental data (red data points) for the non-lasing alexandrite laser amplifier with 4 ms pump pulse and 0.167 mm waist size (experimental black data set of Fig. 5). The model matches the experimental data for the transient pump-induced lens extremely well, with steady-state population lens $D_{P,ss}$ = 16.1 m^{-1}, steady-state thermal lens $D_{T,ss}$ = 6.5 m^{-1}, and thermal time constant t_T = 1.56 ms. The combined pump-induced lens D_{ss} = 22.6 m^{-1} for this modelling is well matched to the experimental steady-state lensing value ~22.5 m^{-1} for this pump power (see Fig. 3). The population component is seen to dominate the lensing. A further independent validation of the high value of population lens is its consistency with the transient pump-probe alexandrite measurement seen in Fig. 4(a) with a large drop in lensing from ~ 21 m^{-1} (non-lasing) to ~ 7 m^{-1} (lasing) when the population lens is clamped.

Further quantitative information on the pump-induced lens was obtained by using a shorter duration pump pulse and using the theoretical analysis for the transient lens growth and decay provided in Section 2. Figure 7 shows the transient pump-induced lensing under non-lasing

Optics EXPRESS

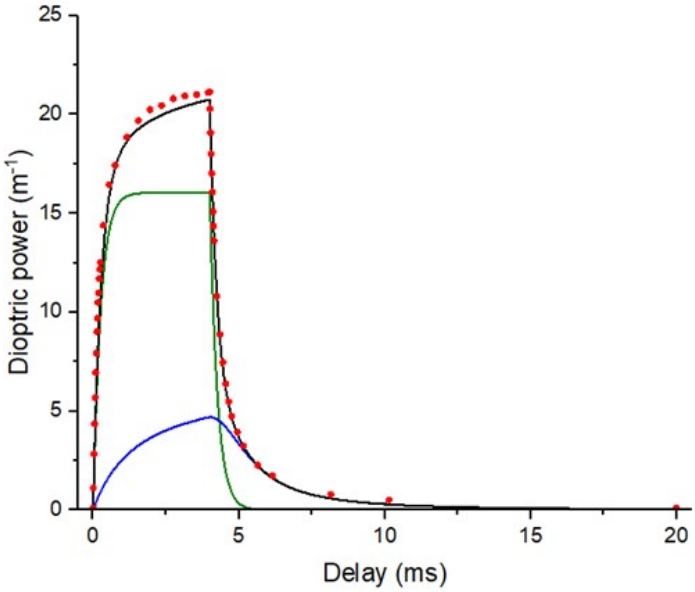


Fig. 6. Modelled transient thermal and population lensing and comparison to experimental pump-induced lensing data for long duration 4 ms pump pulse.

conditions for a short $t_p = 130\ \mu s$ pump pulse with different effective pump waist sizes $w_{p,e} = 0.167$ mm, 0.182 mm, and 0.215 mm, using different pump lenses, f_1.

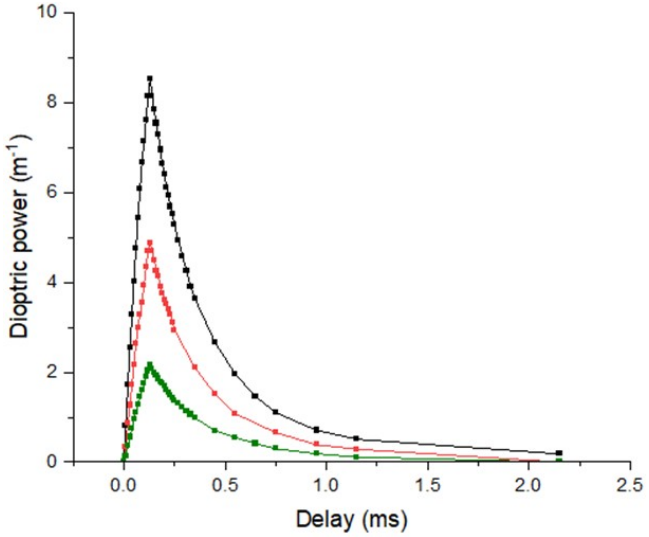


Fig. 7. Transient pump-induced lensing under non-lasing conditions for a short 130 μs pump pulse with different effective pump waist sizes $w_{p,e}$: 0.167 mm (black); 0.182 mm (red); and 0.215 mm (green).

The experimental alexandrite laser amplifier data for the short pump pulse can be made using the model developed in this paper for the transient evolution and decay of the thermal and population lens. The model parameter values used are summarized in Table 2 taken from the

Optics EXPRESS

literature for alexandrite and using the known pump parameters of the experimental system. These values are used as the basis for calculating lensing values based on the analytical theory of Section 2, with no fitting parameters except the factor C that relates the constant of proportionality between the dependence of the refractive index change Δn_p on the fractional inversion given by the relationship in Eq. (14).

Table 2. Alexandrite and pump parameters used in the modelling and data fitting analysis

Parameter	Symbol	Value
Thermal conductivity	κ	23 $Wm^{-1}K^{-1}$
Density	ρ	3690 kgm^{-3}
Specific heat capacity	C_p	1050 $Jkg^{-1}K^{-1}$
Thermal diffusivity	α	5.9 $m^{-2}s^{-1}$
Thermo-optic coefficient (@ 532 nm)	dn/dT	9.1 10^{-6} K^{-1}
Effective thermo-optic coefficient	$(dn/dT)_{eff}$	1.1 10^{-5} K^{-1}
Heat factor (quantum defect)	η_H	0.134
Upper-state heating fraction	β	0.51
Upper-state lifetime (@25°C)	τ	2.6 10^{-4} s
Pump saturation intensity	I_S	1.42 10^{8} Wm^{-2}
Pump absorption coefficient	α_p	560 m^{-1}
Absorbed pump power	P_a	7.47 W
Pump waist size (effective)	$w_{p,e}$	1.67 10^{-4} m
Inversion refractive index coefficient	C	4.5 10^{-5}

The known upper-state lifetime $\tau = 260\ \mu$s for alexandrite at 25°C is used [22]. The pump wavelength is $\lambda_p = 634$ nm, the average spontaneous emission (fluorescence) wavelength in alexandrite is $\lambda_f = 732$ nm [10] which corresponds to a quantum defect heating factor $\eta_H = 0.013$. The upper-laser level has a direct pump band wavelength $\lambda_0 = 680$ nm inferring an upper-level heating fraction $\beta = 0.51$. The thermo-optic coefficient at the probe wavelength 532 nm, is $dn/dT = 9.1\ 10^{-6}\ K^{-1}$ [23], but to include small contributions from surface bulging and photoelastic effect we take a slightly larger (+20%) effective value $(dn/dT)_{eff} = 1.1\ 10^{-5}\ K^{-1}$ [10].

Figure 8 shows the theoretical modelling results of Section 2 for the transient growth (Eq. (16)) and decay (Eq. (18)) of the individual transient thermal lens $D_T(t)$ (blue curve) and population lens $D_P(t)$ (green curve), and the combined lens $D(t)$ (black curve) for short pump pulse duration 130 µs with 0.167 mm effective pump waist size (the case for the black data set in experimental graph of Fig. 7).

The theoretical combined lens has good matching to the experimental data (red data points). The thermal time constant $t_0 = 600\ \mu s$ is calculated from Eq. (9) in this case. In the growth phase, the population lens is seen to be dominant with a faster growth rate than the thermal lens component during the build-up phase of the pumping pulse. In the decay phase, the population lens decays at with a faster (exponential) upper-state lifetime, $\tau = 260\ \mu s$ than the thermal lens at slower rate (non-exponential) time constant $t_0 = 600\ \mu s$. A good match to the experimental data is found with inversion refractive index coefficient $C = 4.5\ 10^{-5}$. This value is consistent with a calculated value $C = 4.75\ 10^{-5}$ based on the linearity of steady-state dioptric power with absorbed pump power when account of excited state absorption is included [10]. The analytical model predicts steady-state population and thermal lensing powers are $D_{P,ss} = 20.2\ m^{-1}$ and $D_{T,ss} = 5.5\ m^{-1}$, respectively, based on an idealized four-level amplifier system.

Optics EXPRESS

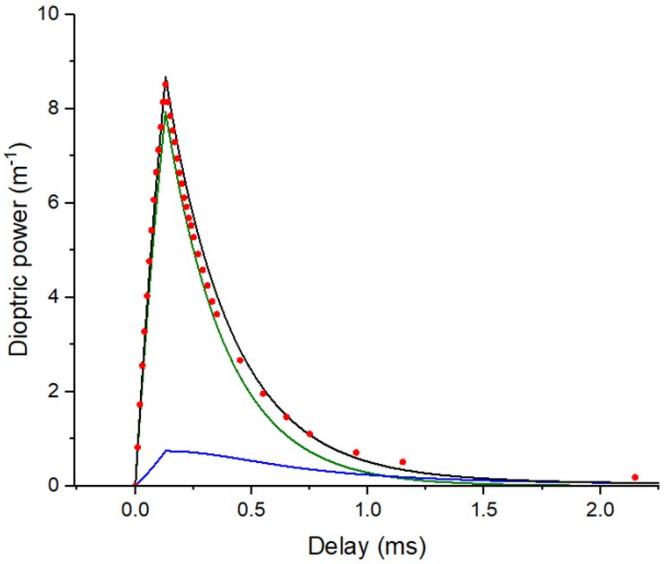


Fig. 8. Modelled transient build-up and decay of thermal (blue) and population (green) lensing and comparison of theoretical combined lens (black) with experimental data for measured pump-induced lens (red data points) for short duration 130 µs pump pulse.

5. Discussion

The results of the theoretical modelling fit very well both in qualitative trend and quantitative agreement with transient pump-probe experiments of pump-induced lensing in the alexandrite gain medium. The comparison with a simple analytical theory of this paper provides quantitative information on the relative contribution of the thermal and population lenses and their transient growth and decay. A related experimental technique of transient pump-induced lensing measurement was used recently in a transversely-pumped Nd:YAG rod [24]. The interpretation of the results in that study, however, required complicated COMSOL numerical modelling of the heat diffusion equation and assumptions of the transverse heating profile. Their measured lensing modulation was just a few percent on a large steady-state background lens due to the long thermal time constant resulting from the large transverse extent of the heating profile. With the Gaussian end-pumping pulse methodology of this paper, the heating profile is known, and its size was also able to be readily varied. The small transverse pump size of this end-pumped case, is shown to allow almost complete erasure of the thermal lens between pulses, giving a simpler modelling analysis of single pump pulse without persistent background lensing effects, using repetitive pulsing required for the delayed probe experimental procedure.

The theoretical modelling in this paper is based on an ideal four-level system. However, alexandrite is known to have excited-state absorption (ESA) for the pump beam [10,25,26]. At high inversions of the gain medium, ESA leads to an additional heating factor which would increase the thermal lens component, and inversion saturation leads to a reduced population lens. This trend is seen in the difference in modelled values of steady-state population and thermal lenses for short and long pump pulses The analytical prediction with the short 130 µs pump pulse (when inversions are lower and closer to ideal four-level behaviour) gives $D_{P,ss}$ = 20.2 m^{-1} and $D_{T,ss}$ = 5.5 m^{-1}, respectively. This can be compared to the long 4 ms pump pulse (when inversion is highest, and ESA and saturation strongest) where modelled fitting to experimental results predicts lower population lens $D_{P,ss}$ = 16.1 m^{-1} and higher thermal lens $D_{T,ss}$ = 6.5 m^{-1}.

Optics EXPRESS

It is noted that the lensing measurement is the refractive index distribution perceived by the probe beam which was at 532 nm in this study. The thermal component of the pump-induced lens for the laser wavelength (~ 760 nm, in alexandrite) should be modified as the thermo-optic coefficient has a slightly lower value $dn/dT \sim 7.5\ 10^{-6}\ \mathrm{K}^{-1}$ at ~ 760 nm than its value $dn/dT = 9.1\ 10^{-6}\ \mathrm{K}^{-1}$ at probe wavelength 532 nm [23]. The polarization lens factor $C(\lambda)$ may also need some modification if the polarizability difference between excited and ground state is wavelength-dependent. In V. Pilla's study, they measured the polarizability difference at 514 nm of alexandrite as $\Delta\alpha_p = 2.7\ 10^{-31}\ cm^3$ [27]. A probe beam at the laser wavelength can be used to establish the wavelength dependence of the lensing although it is harder to spectrally separate the probe from the spontaneous or stimulated emission from the inverted amplifier.

In the analysis of this paper, it is assumed that every absorbed pump photon produces an upper-level population (pump quantum efficiency, $\eta_Q = 1$) and all upper-level population decays radiatively without non-radiative routes (radiative quantum efficiency, $\eta_r = 1$). These quantum efficiency factors can be readily included but for brevity are not considered in this analysis, as these are equal (or close to equal) to unity in alexandrite [22] as well as in most commonly-used gain media.

6. Conclusions

A transient analysis has been developed of pump-induced lensing in a laser amplifier with combined thermal and population components in an end-pumped laser amplifier by a pulsed pump beam with Gaussian intensity distribution. Whilst incorporating physical mechanisms well-known in the literature for pump-induced lensing, to our knowledge, the analysis of this paper develops new features of the transient development of the thermal lens based on the solution of the heat-diffusion equation for a delta-function heating impulse and the analysis provides the rigorous incorporation in the lensing analysis of two-step heating from the four-level amplifier with time-delayed heating component following spontaneous emission. Transient pump-probe measurements have been made of the pump-induced lensing in an alexandrite gain medium under end-pumping by a pulsed Gaussian pump beam and short-pulse probe with a time-gated Shack-Hartmann wavefront sensor to provide high temporal resolution of the growth and decay of the induced lensing.

The modelling results of the transient pump-analysis show excellent agreement in qualitative trend and quantitative correspondence with experimental lensing results for short pumping pulse duration, and with fitting to longer pumping pulse when evolution towards quasi-steady-state lensing is reached. The transient results confirm unambiguously the presence of a strong population component to the pump-induced lens in red-diode-pumped alexandrite that is demonstrated to be considerably stronger than the thermal lens. Varying pump size is shown to change the relative contribution of the population lens, which is largest for smallest pumping beam size, in correspondence to our theoretical prediction. Experimental measurement of the transient lens under lasing conditions provides insight into the significant decrease in the lensing strength compared to the non-lasing case. This difference is well-explained and quantified in this study by the presence of the large population lens component under non-lasing conditions that is clamped to a low value under lasing conditions. The full transient evolution of the lensing at the onset of lasing is also clearly able to be monitored by our transient pump-probe methodology.

The transient experiment and theoretical modelling on pump-induced lensing in alexandrite in this work provides useful insight for future pulsed pumping experiments for Q-switched alexandrite laser operation which is an active and attractive prospect for atmospheric and vegetation remote sensing lidar [28,29]. The fast response of the population lens to inversion change is also the likely mechanism for self-Q-switching that has been observed in alexandrite [16] and in the related material Cr:LiCAF [15]. The transient analysis of this paper can be used

Optics EXPRESS

as a basis to model the self-Q-switching mechanism and to optimize its performance or to avoid its occurrence.

Alexandrite is known to have excited-state absorption (ESA) for the pump beam [25,26] that will provide additional heating. The effect of ESA heating and inversion saturation is consistent with the trend in population and thermal lens components of our modelling results between the short pump pulse (low inversion case) and long pump pulse (high inversion case). The consideration of ESA heating factor and population inversion saturation will be the subject of a future paper on alexandrite with more extensive transient pump-probe experiments including with a blue pump with higher quantum defect heating, using different crystal temperatures which changes the upper-state lifetime in alexandrite, and pumping of plane-plane and Brewster-cut crystal geometries.

Whilst this study focused experimentally on the alexandrite gain medium, the theory and experimental methodology developed in this paper should be able to be successfully applied more generally to other gain media and possibly also (non-gain) optical media with residual absorption at the pump laser wavelength. We therefore believe the methods employed in this paper will be beneficial to serve the community to understand, control and develop future laser technology.

Funding. European Space Agency (4000115840/15/NL/PA/zk).

Acknowledgment. The authors thank Dr A. Minassian for technical assistance, and Martin Kehoe and Simon Johnson for manufacture of mechanical workshop parts.

Disclosures. The authors declare no conflicts of interest.

Data availability. Data underlying the results presented in this paper are not publicly available at this time but may be obtained from the authors upon reasonable request.

References

1. W. Koechner, *Solid-state laser engineering* (Sringer, 2006, 6th ed.).
2. S. Chenais, F. Balembois, F. Druon, *et al.*, "Thermal lensing in diode-pumped ytterbium laser – Part 1: theoretical analysis and wavefront measurements," IEEE J. Quantum Electron. **40**(9), 1217–1234 (2004).
3. O. Antipov, A. S. Kuzhelev, D. V. Chausov, *et al.*, "Dynamics of refractive-index changes in a Nd:YAG laser crystal under excitation of Nd^{3+} ions," J. Opt. Soc. Am. B **16**(7), 1072–1079 (1999).
4. O. Antipov, O. Eremeykin, A. Savikin, *et al.*, "Electronic changes of refractive index in intensively pumped Nd:YAG laser crystals," IEEE J. Quantum Electron. **39**(7), 910–918 (2003).
5. L. Freitas, C. Jacinto, A. Rodenas, *et al.*, "Time-resolved study electronic and thermal contributions to the nonlinear refractive index of Nd3+:SBN laser crystals," J. Lumin. **128**(5-6), 1013–1015 (2008).
6. R. Soulard, A. Zinoviev, J. L. Doualan, *et al.*, "Detailed characterization of pump-induced refractive index changes observed in Nd:YVO_4, Nd:$GdVO_4$ and Nd:KGW," Opt. Express **18**(2), 1553–1568 (2010).
7. A. Andrade, E. Tenorio, T. Catunda, *et al.*, "Discrimination between electronic and thermal contributions to the nonlinear refractive index of SrAlF5:Cr3+," J. Opt. Soc. Am. B **16**(3), 395–400 (1999).
8. N. Passilly, E. Haouas, V. Ménard, *et al.*, "Population lensing effect in Cr:LiSAF probed by Z-scan technique," Opt. Commun. **260**(2), 703–707 (2006).
9. T. Godin, R. Moncorgé, J.-L. Doualan, *et al.*, "Optically pump-induced athermal and nonresonant refractive index changes in the reference Cr-doped laser materials: Cr:GSGG and ruby," J. Opt. Soc. Am. B **29**(5), 1055–1064 (2012).
10. G. Tawy, J. Wang, and M.J. Damzen, "Pump-induced lensing effects in diode pumped Alexandrite lasers," Opt. Express **27**(24), 35865–35883 (2019).
11. G. Tawy, J. Wang, and M.J. Damzen, "Population lensing in Alexandrite lasers," OSA Technical Digest, CLEO-Europe, Munich, paper ca_p_11 2019
12. R. Moncorgé, O. Eremeykin, J. Doualan, *et al.*, "Origin of athermal refractive index changes observed in Yb3 + doped YAG and KGW," Opt. Commun. **281**(9), 2526–2530 (2008).
13. O. L. Antipov, D. V. Bredikhin, O. N. Eremeykin, *et al.*, "Electronic mechanism for refractive-index changes in intensively pumped Yb:YAG laser crystals," Opt. Lett. **31**(6), 763–765 (2006).
14. M. Kilinc, U. Demirbas, J. B. Gonzalez-Diaz, *et al.*, "Thermal and population lensing of Yb:YLF at cryogenic temperature," Opt. Mater. Express **13**(11), 3200–3216 (2023).
15. E. Beyalti, A. Sennaroglu, and U. Demirbas, "Self-Q-switched Cr:LiCAF laser," J. Opt. Soc. Am. B **30**(4), 914–920 (2013).
16. G. Tawy and M. J. Damzen, "Tunable, dual wavelength and self-Q-switched Alexandrite laser using crystal birefringence control," Opt. Express **27**(13), 17507–17520 (2019).
17. S. Chenais, F. Druon, S. Forget, *et al.*, "On thermal effects in solid-state lasers: the case of ytterbium-doped materials," Prog. in Quantum Electron. **30**(4), 89–153 (2006).

Optics EXPRESS

18. B. Neuenschwander, R. Weber, and H. P. Weber, "Determination of the thermal lens in solid-state lasers with stable cavities," IEEE J. Quantum Electron. **31**(6), 1082–1087 (1995).
19. J. L. Blows, J. M. Dawes, and T. Omatsu, "Thermal lensing measurements in line-focus end-pumped neodymium yttrium aluminium garnet using holographic lateral shearing interferometry," J. Appl. Phys. **83**(6), 2901–2906 (1998).
20. L. D. Landau and E.M. Lifshitz, "*Fluid Mechanics*", 2nd Ed, Pergamon Press, Oxford 1987
21. S. Chenais, F. Balembois, F. Druon, *et al.*, "Thermal lensing in diode-pumped ytterbium laser – Part II: evaluation of quantum efficiencies and thermo-optic coefficients," IEEE J. Quantum Electron. **40**(9), 1235–1243 (2004).
22. J. Walling, O. Peterson, H. Jenssen, *et al.*, "Tunable alexandrite lasers," IEEE J. Quantum Electron. **16**(12), 1302–1315 (1980).
23. P. Loiko, S. Ghanbari, V. Matrosov, *et al.*, "Dispersion and anisotropy of thermo-optical properties of alexandrite laser crystal," Opt. Mater. Express **8**(10), 3000–3006 (2018).
24. M. Maillard, G. Amiard-Hudebine, M. Tondusson, *et al.*, "Kinetics and wavelength dependence of thermal and excited-state population on lens effect induced in a Nd:YAG rod amplifier," Opt. Express **31**(2), 1799–1812 (2023).
25. M. Shand and H. Jenssen, "Temperature dependence of the excited-state absorption of alexandrite," IEEE J. Quantum Electron. **19**(3), 480–484 (1983).
26. W. R. Kerridge-Johns and M. J. Damzen, "Analysis of pump excited state absorption and its impact on laser efficiency," Laser Phys. Lett. **12**(12), 125002 (2015).
27. V. Pilla, P. R. Impinnisi, and T. Catunda, "Measurement of saturation intensities in ion doped solids by transient nonlinear refraction," Appl. Phys. Lett. **70**(7), 817–819 (1997).
28. G. M. Thomas, A. Minassian, X. Sheng, *et al.*, "Diode-pumped alexandrite lasers in q-switched and cavity-dumped q-switched operation," Opt. Express **24**(24), 27212–27224 (2016).
29. A. Munk, M. Strotkamp, M. Walochnik, *et al.*, "Diode-pumped q-switched alexandrite laser in single longitudinal mode operation with watt-level output power," Opt. Lett. **43**(22), 5492–5495 (2018).

146.179.86.58 {ts '2024-03-22 10:56:50'}